MHC II$^+$ resident peritoneal and pleural macrophages rely on IRF4 for development from circulating monocytes

Ki-Wook Kim,[1] Jesse W. Williams,[1] Ya-Ting Wang,[1] Stoyan Ivanov,[1] Susan Gilfillan,[1] Marco Colonna,[1] Herbert W. Virgin,[1] Emmanuel L. Gautier,[2] and Gwendalyn J. Randolph[1]

[1]Department of Pathology and Immunology, Washington University School of Medicine, St. Louis, MO 63110
[2]Institut National de la Santé et de la Recherche Médicale UMR_S 1166, Sorbonne Universités, Université Pierre-et-Marie-Curie (UPMC) Paris 06, Pitié-Salpêtrière Hospital, 75013 Paris, France

Peritoneal and pleural resident macrophages in the mouse share common features and in each compartment exist as two distinct subpopulations: F4/80$^+$ macrophages and MHC II$^+$ CD11c$^+$ macrophages. F4/80$^+$ macrophages derive from embryonic precursors, and their maintenance is controlled by Gata6. However, the origin and regulatory factors that maintain MHC II$^+$ macrophages remain unknown. Here, we show that the MHC II$^+$ macrophages arise postnatally from CCR2-dependent precursors that resemble monocytes. Monocytes continuously replenish this subset through adulthood. Gene expression analysis identified distinct surface markers like CD226 and revealed that the transcription factor IRF4 was selectively expressed in these macrophages relative to other organs. Monocytes first entered peritoneal or pleural cavities to become MHC II$^+$ cells that up-regulated CD226 and CD11c later as they continued to mature. In the absence of IRF4 or after administration of oral antibiotics, MHC II$^+$CD226$^-$CD11c$^-$ monocyte-derived cells accumulated in peritoneal and pleural cavities, but CD11c$^+$ CD226$^+$ macrophages were lost. Thus, MHC II$^+$ resident peritoneal and pleural macrophages are continuously replenished by blood monocytes recruited to the peritoneal and pleural cavities constitutively, starting after birth, where they require IRF4 and signals likely derived from the microbiome to fully differentiate.

INTRODUCTION

Macrophages can be classified into two broad groups according to whether they originate from embryonic precursors or adult blood monocytes (Lavin et al., 2015; Ginhoux and Guilliams, 2016). Most peripheral tissues contain a dominant resident macrophage population that is maintained by local self-proliferation without relying on circulating monocytes to be replenished (Schulz et al., 2012; Hashimoto et al., 2013; Yona et al., 2013). In addition, there is often a second, quantitatively more minor resident macrophage subpopulation, such as that described in the heart (Epelman et al., 2014a,b; Molawi et al., 2014), lung (Schneider et al., 2014), liver (Yona et al., 2013), skin (Tamoutounour et al., 2013), and peritoneum (Ghosn et al., 2010). Whether there is a common relationship between the two macrophage populations within a given organ remains unclear. In some instances, the second population may be a transitional stage for the major population and simply appear phenotypically distinct. However, in some organs like skin and heart, one population appears to be derived from local proliferation and another from circulating precursors (Tamoutounour et al., 2013; Epelman et al., 2014b; Molawi et al., 2014). Furthermore, in the liver, the two subpopulations occupy distinct anatomical niches (Yona et al., 2013).

Here, we extended recent studies on resident peritoneal macrophages to consider the second resident peritoneal macrophage population. Peritoneal macrophages, and pleural macrophages that resemble them (Rosas et al., 2014), are divided into two distinct populations based on size and phenotype, originally referred to as large and small peritoneal macrophages, with terms large and small referring both to cell size and relative frequency (Ghosn et al., 2010). Large peritoneal macrophages express high F4/80, whereas small macrophages highly express MHC II and low F4/80. They also express CD11c, which led us in the past to wonder if they were closely related to DCs, but profiling studies clearly classified them as macrophages (Gautier et al., 2012). The transcription factor Gata6 is crucial for maintenance of homeostasis in the F4/80$^+$ large macrophage subpopulation within the peritoneal or pleural microenvironment (Gautier et al., 2012, 2014; Okabe and Medzhitov, 2014; Rosas et al., 2014). Yet, the small MHC II$^+$ macrophage subset that resides in the same microenvironment neither expresses nor depends on Gata6. We thus considered the possibility that it was apparently unaffected by the absence of Gata6 because it simply served as a transient precursor for the Gata6$^+$ macrophage, as previously proposed (Cain et al., 2013). We therefore set out herein to better understand the life cycle of the small resident peritoneal macrophage.

Correspondence to Gwendalyn J. Randolph: grandolph@path.wustl.edu

The Rockefeller University Press $30.00
J. Exp. Med. 2016 Vol. 213 No. 10 1951–1959
www.jem.org/cgi/doi/10.1084/jem.20160486

RESULTS AND DISCUSSION

MHC II$^+$ macrophages are distinguished by CD226 expression in peritoneal and pleural cavities

All peritoneal and pleural macrophages express CD115 (*Csf1r*) and CD11b (*Itgam*). These macrophages can be divided into Gata6-dependent F4/80$^+$ ICAM2$^+$ large macrophages and Gata6-independent F4/80^{lo} MHC II$^+$ small macrophages. Consistent with predictions stemming from gene expression profiling (Fig. 1 A and Table S1), CD226, also known as DNAX accessory molecule-1 (DNAM-1), was selectively expressed on MHC II$^+$ macrophages but not on F4/80$^+$ ICAM2$^+$ macrophages in peritoneum and pleura or on macrophages elsewhere (Fig. 1, A and B). Blood monocytes expressed CD226 weakly if not at all (Fig. 1 B). Peritoneal F4/80$^+$ ICAM2$^+$ macrophages comprised >90% and MHC II$^+$ macrophages comprised <10% of total macrophages in the peritoneum, respectively (Fig. 1 C). Although most MHC II$^+$ macrophages expressed CD226, a remnant consisting of <15% of this macrophage subset did not express CD226 (Fig. 1 C). Similar results were observed in the pleural cavity (Fig. 1 D). As expected (Gautier et al., 2012), flow cytometric analysis revealed high levels of CD11c on CD226$^+$ peritoneal macrophages, but not F4/80$^+$ ICAM2$^+$ macrophages (Fig. 1 E). In CD11c-EYFP reporter mice, EYFP was homogeneously expressed on CD226$^+$ macrophages but not on the CD226$^-$ macrophages within the MHC II$^+$ macrophage subpopulation (Fig. 1 F), nor on blood monocytes (Fig. 1 G). To investigate whether MHC II$^+$ CD226$^-$ macrophages were similar to Ly6C^{hi} or Ly6C^{lo} blood monocytes, we analyzed the expression of a panel of blood monocyte markers. MHC II$^+$ macrophages were GFP$^+$ in CCR2-GFP mice (Fig. 1 H), indicating recent expression of CCR2, but they lacked the expression of Ly6C that marks most blood CCR2$^+$ monocytes (Fig. 1 H). Whereas Ly6C^{lo} monocytes expressed TremL4 (Ingersoll et al., 2010), MHC II$^+$ CD226$^-$ macrophages did not. Thus, MHC II$^+$ CD226$^-$ macrophages did not directly overlap in phenotype with Ly6C^{hi} monocytes or Ly6C^{lo} monocytes, but did share monocyte properties (Fig. 1 H). We thus wondered whether the CD226$^-$ fraction of MHC II$^+$ macrophages might derive from monocytes and whether these CD226$^-$ cells in turn might serve as precursors for the CD226$^+$ MHC II$^+$ macrophages that comprised the majority of this subpopulation.

CD226$^+$ resident macrophages develop postnatally

To investigate whether MHC II$^+$ macrophages derive from infiltrating monocytes, we analyzed cells from peritoneal lavage of CD11c-EYFP pups, starting after birth (P0) through postnatal day 12 (P12). In this early period, we observed three distinct populations; F4/80$^+$ ICAM2$^+$ macrophages corresponding to the major subset of resident macrophages (Gautier et al., 2012) and ICAM2$^-$ macrophages that were MHC II$^+$ or MHC II^{lo} (Fig. 2 A). The finding of F4/80$^+$ ICAM2$^+$ macrophages in newborn mice supports the conclusion that they are seeded before birth (Hashimoto et al., 2013; Yona et al., 2013). Although ICAM2$^-$ MHC II$^+$ macrophages were detected between P0 and P2, CD226$^+$ macrophages were not. They were first detected between P4 and P6, progressively increasing so that by P12 the frequency observed in adult was reached (compared Fig. 2 [B and C] with Fig. 1 C). In contrast, the population of MHC II^{lo} ICAM2$^-$ cells was proportionally more prominent in the first few days after birth than any later time. These MHC II^{lo} cells, analyzed from P4 pups, expressed high Ly6C and were uniformly GFP$^+$ in CX$_3$CR1$^{gfp/+}$ mice (Fig. 2 D), indicating that the MHC II^{lo} cells were similar to monocytes (Geissmann et al., 2003) and may arise from monocytes recruited to the perinatal peritoneal cavity. Similar to adult mice (Fig. 1 F), EYFP expression in CD11c-EYFP pups was homogeneously expressed on MHC II$^+$ CD226$^+$ macrophages but not on the MHC II^{lo} population (Fig. 2 E), again consistent with the fact that Ly6C^{hi} monocytes do not express CD11c (Ingersoll et al., 2010). Between P0 and P8, MHC II$^+$ CD226$^-$ macrophages heterogeneously expressed EYFP (Fig. 2 E) and were heterogeneous for GFP expression in CX$_3$CR1$^{gfp/+}$ mice (Fig. 2 D). However, after the emergence of CD226$^+$ macrophages that peaked by P12–14, few EYFP$^+$ MHC II$^+$ CD226$^-$ cells were detectable (Fig. 2 E). We wondered whether this was because their conversion to EYFP$^+$ MHC II$^+$ CD226$^+$ macrophages was occurring rapidly by P12 (Fig. 2 E). These data are consistent with the possibility that both CD11c^{hi} CD226$^+$ macrophages are replenished through MHC II$^+$ CD11c$^-$ CD226$^-$ precursors that in turn arise from Ly6C^{hi} MHC II^{lo} monocytes. The earlier appearance and close resemblance of CD226$^-$ macrophages to blood Ly6C^{hi} monocytes suggest a possible model in which monocytes are first recruited into the peritoneum to become CD226$^-$ macrophages that serve as intermediates to more differentiated CD226$^+$ macrophages.

CD226$^+$ macrophages are continuously replenished from circulating CCR2$^+$ monocytes

If MHC II$^+$ macrophages are derived from Ly6C^{hi} monocytes, reductions in blood Ly6C^{hi} monocytes would be expected to reduce the number of CD11c^{hi} CD226$^+$ macrophages or MHC II$^+$ CD226$^-$ macrophages. Accordingly, we examined the peritoneal MHC II$^+$ macrophages in CCR2-deficient mice in which Ly6C^{hi} monocytes do not efficiently enter blood from bone marrow (Serbina and Pamer, 2006). As expected (Newson et al., 2014; Okabe and Medzhitov, 2014), F4/80$^+$ peritoneal macrophages were not affected by CCR2 deficiency. However, MHC II$^+$ macrophages were markedly reduced in CCR2-deficient mice (Fig. 3 A), including both MHC II$^+$ CD226$^-$ macrophages and CD226$^+$ macrophages (Fig. 3 B), suggesting that both are downstream of a CCR2-dependent precursor, likely the Ly6C^{hi} monocyte.

Monocyte expression of CX$_3$CR1 allows them to be studied in fate mapping experiments using CX$_3$CR1^{CreER} mice (Yona et al., 2013). To further investigate whether circulating cells like monocytes may contribute to the maintenance of peritoneal CD226$^+$ macrophages in adult mice, we set up fate

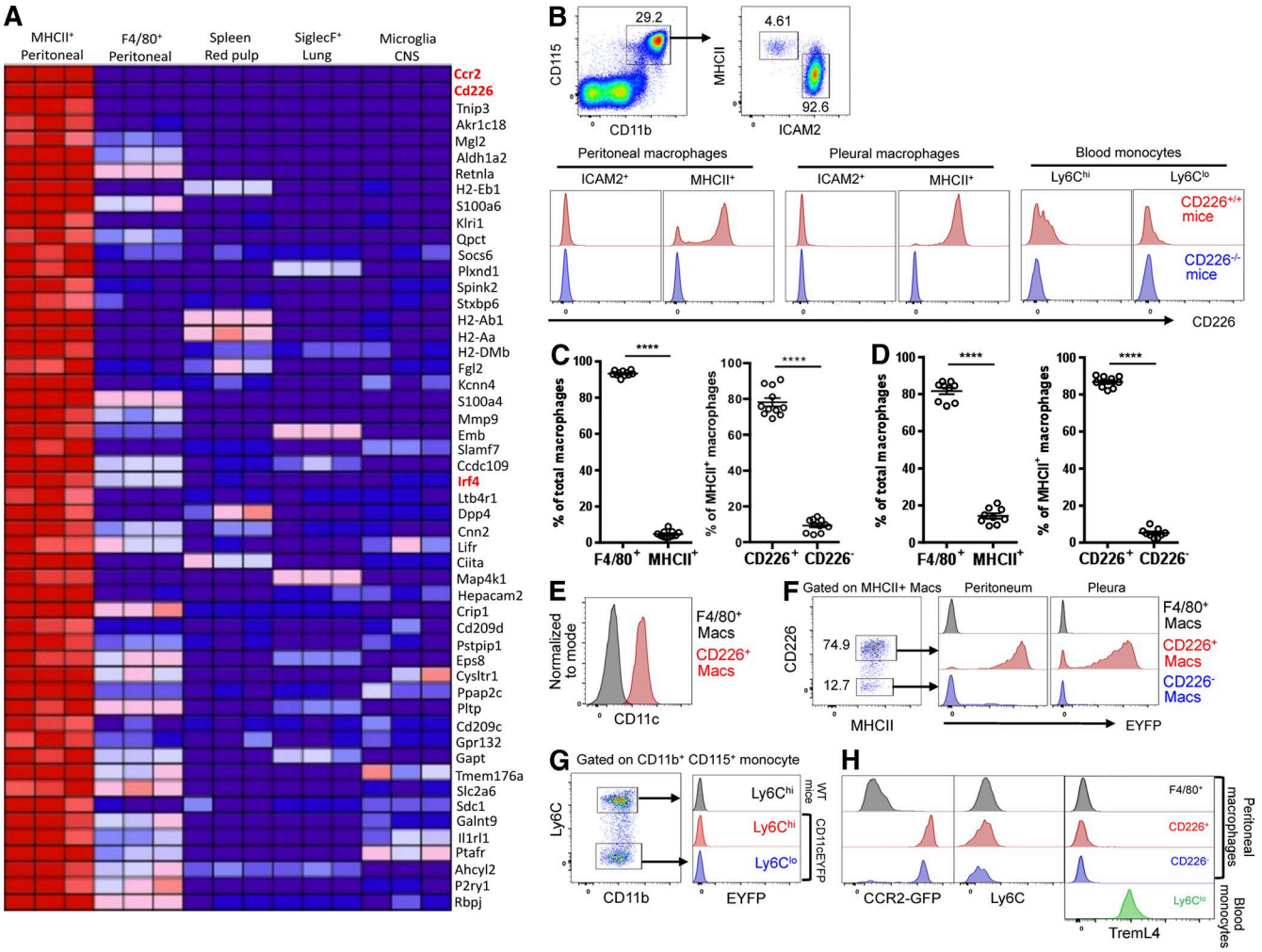

Figure 1. **MHC II$^+$ macrophages divide into CD226$^+$ and CD226$^-$ subpopulations in peritoneum and pleura.** (A) Heat map depicts mean expression intensity of mRNA transcripts for genes differentially expressed between MHC II$^+$ peritoneal macrophages and other macrophages. Transcripts highlighted in red text are those studied in this body of work. Cut-off for depiction includes transcripts expressed more than fivefold in MHC II$^+$ versus F4/80$^+$ ICAM2$^+$ peritoneal macrophages. (B) Gating strategy used for identification of peritoneal macrophages (top dot plot panels) and histograms of CD226 expression on F4/80$^+$ ICAM2$^+$ and MHC II$^+$ macrophages or blood monocytes (bottom panels). (C and D) Quantification of macrophages in B in peritoneum (C) or pleural cavity (D). Data are combined from three independent experiments (n = 9–11, mean ± SEM). P-values, unpaired Student's t test: ****, P < 0.0001. (E) CD11c expression on peritoneal F4/80$^+$ and CD226$^+$ macrophage subpopulations. (F and G) EYFP expression in CD11c-EYFP mice within MHC II$^+$ macrophage subpopulations in peritoneum and pleura (F) or within blood monocytes (G). Data are representative of at least three independent experiments. (H) CCR2-GFP, Ly6C, and TremL4 expression in peritoneal macrophage subpopulations or Ly6C^{lo} blood monocytes. Data are representative of three independent experiments.

mapping experiments using CX_3CR1^{CreER} × $Rosa26^{TdTomato}$ mice. Tamoxifen was given in the diet for 3 wk, and then animals were analyzed for reporter expression in peritoneal and pleural macrophages. As expected (Yona et al., 2013), Tomato reporter poorly labeled F4/80$^+$ ICAM2$^+$ peritoneal (1.2 ± 0.2%) and pleural macrophages (6.2 ± 0.8%; Fig. 3 C). However, most CD226$^+$ macrophages were positive for Tomato reporter in the peritoneal (89 ± 1.5%) and pleural cavity (88 ± 1.6%). Similar to CD226$^+$ macrophages, MHC II$^+$ CD226$^-$ macrophages were efficiently labeled by Tomato reporter in peritoneum (79 ± 3.1%) and pleura (86 ± 4.0%). The proportion of Tomato labeling was significantly increased in both CD226$^+$ macrophages and MHC II$^+$ CD226$^-$ macrophages, compared with the Tomato expression of Ly6C^{hi} monocytes (67 ± 1.6%; Fig. 3 C). Because reporter expression is slightly delayed in comparison with the induction of the gene driving Cre, the progressive increase in reporter expression from monocytes to CD226$^-$ MHC II$^+$ to CD226$^+$ MHC II$^+$ macrophages might imply a progressive developmental relationship between all of these CCR2-dependent cells. Alternatively, CX_3CR1 expression might be up-regulated in MHC II$^+$ macrophages as they reside in the visceral cavities. To distinguish these possibilities,

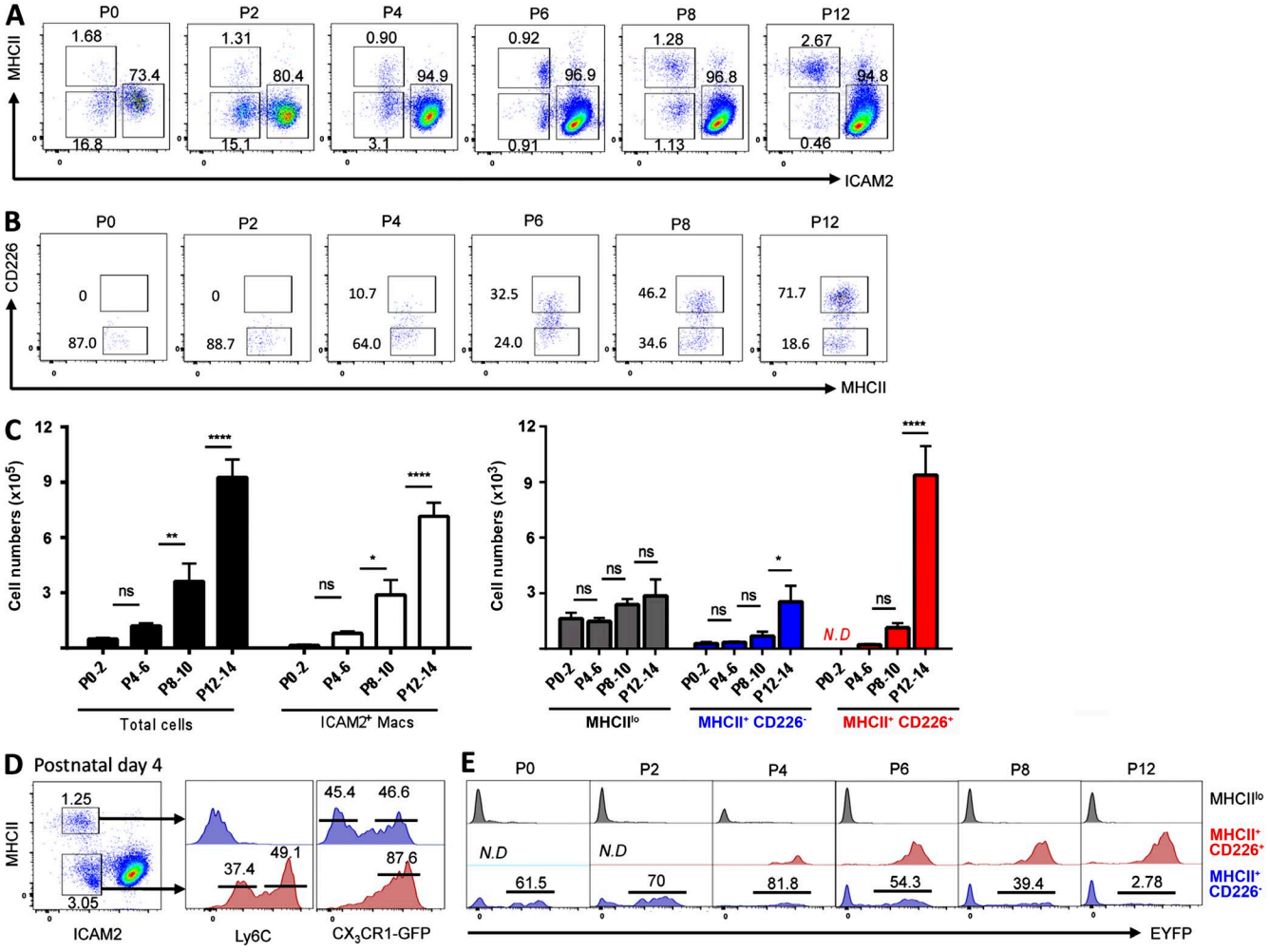

Figure 2. **CD226⁺ macrophages develop after birth.** (A and B) Peritoneal cells after pregating CD11b⁺ CD115⁺ macrophages (A) and the MHC II⁺ macrophage subpopulation (B) from P2, P4, P6, P8, or P12 in CD11c-EYFP mice. (C) Quantification of total cell, F4/80⁺ICAM2⁺, MHC II^{lo}, or MHC II⁺ macrophage subpopulations shown in A and B. P-values from multiple comparisons of two-way ANOVA: *, $P < 0.05$; **, $P < 0.01$; ****, $P < 0.0001$. Mean ± SEM. (D) Ly6C and GFP expression on MHC II⁺ and MHC II^{lo} cells from P4 in $CX_3CR1^{gfp/+}$ mice. Data are the representative of two independent experiments ($n = 3$ mice/experiment). (E) EYFP expression by MHC II^{lo} cells, CD226⁺ macrophages, and MHC II⁺ CD226⁻ macrophages in CD11c-EYFP mice. (A–C and E) Data are pooled from at least four independent experiments (P0–2, $n = 8$ mice; P4–6, $n = 8$ mice; P8–10, $n = 4$ mice; P12–14, $n = 4$ mice).

we analyzed MHC II⁺ macrophages in $CX_3CR1^{gfp/+}$ mice. GFP was expressed on most MHC II⁺ CD226⁻ macrophages in peritoneum (84 ± 4.2%) and pleura (92 ± 3.4%). However, GFP expression by CD226⁺ macrophages in $CX_3CR1^{gfp/+}$ mice was significantly reduced in the peritoneum (41 ± 1.2%), consistent with previous work (Cain et al., 2013), and pleura (47 ± 1.6%; Fig. 3 D). Thus, we conclude that CX_3CR1 expression is down-regulated during the differentiation of CD226⁺ macrophages, once CX_3CR1^+-expressing precursors arrive in the peritoneal or pleural cavity from blood. These data, together with the analysis in CCR2-deficient mice, support the model developed from examination of the peritoneal cavity after birth in which monocytes are recruited into the peritoneum and progressively differentiate into MHC II⁺ CD226⁻ macrophages and then finally into MHC II⁺ CD226⁺ macrophages.

To further test whether CD226⁺ macrophages may derive from blood monocytes, we established parabiotic pairs between CD45.2 CD11c-EYFP and CD45.1 WT mice. 2 mo after the surgery, T cells (46 ± 5%) and B cells (42 ± 3%) in peritoneum were equally distributed between parabiotic pairs. However, as expected, Ly6C^{hi} monocytes were only partially equilibrated in this 2-mo period (Liu et al., 2009), and F4/80⁺ ICAM2⁺ macrophages in both peritoneum and pleura showed only 2.2 ± 1.7% chimerism and 8.9 ± 5.1% chimerism, respectively, again as expected (Hashimoto et al., 2013). CD226⁺ macrophages exchanged to 19 ± 6.4% in peritoneum and 22.6 ± 7.6% in pleura, closely corresponding to the exchange between circulating Ly6C^{hi} monocytes (Fig. 3 E). Finally, adoptive transfer of monocytes i.v. revealed that monocytes entered the peritoneal cavity and became

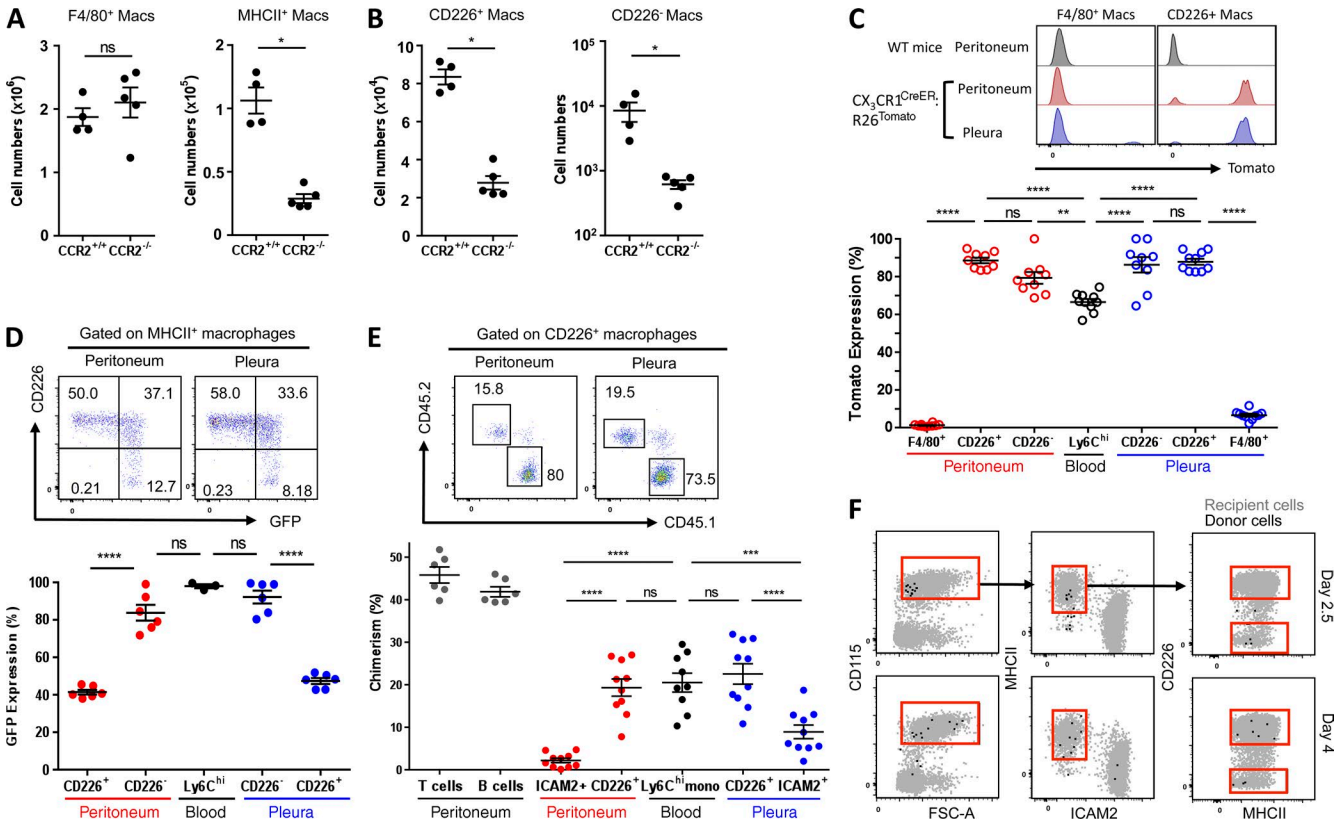

Figure 3. **CD226⁺ macrophages are replenished by circulating monocytes.** (A and B) Quantification of peritoneal F4/80⁺ ICAM2⁺ or MHC II⁺ macrophages (A) or CD226⁺ or CD226⁻ subsets of MHC II⁺ macrophages (B) in CCR2$^{+/+}$ and CCR2$^{-/-}$ mice. Data are from three independent experiments (n = 4–5 mice/genotype, mean ± SEM). P-values, unpaired Student's t test: *, P < 0.05. (C) Representative histogram and the quantification (graph just beneath the histogram) of Tomato reporter expression within F4/80⁺ macrophages and MHC II⁺ macrophage subpopulations in both peritoneum and pleura from tamoxifen-treated CX$_3$CR1^{CreER} × Rosa26^{Tomato} mice. Data are pooled from three independent experiments (n = 9–10 mice per group, mean ± SEM). (D) CX$_3$CR1 expression and its quantification on peritoneal and pleural F4/80⁺, CD226⁺, and MHC II⁺ CD226⁻ macrophages as assessed in CX$_3$CR1$^{gfp/+}$ mice. Data are combined from two independent experiments (n = 3–6 mice per group, mean ± SEM). (E) Representative flow cytometric analysis of CD45.2 expression on CD226⁺macrophages in peritoneum and pleura from the CD45.1-expressing parabiont during parabiosis and the chimerism from CD45.1:CD45.2 CD11cEYFP parabiotic mice. Data are pooled from three independent experiments (n = 6–10, mean ± SEM). (C–E) P-values, multiple comparisons in one-way ANOVA: **, P < 0.01; ***, P < 0.001; ****, P < 0.0001. (F) Peritoneal cell analysis of congenic CD45.1 recipient mice at day 2.5 and day 4 after adoptive transfer of monocyte from CD45.2 CCR2$^{gfp/+}$ mice. Pregated on CD45.2⁺ GFP⁺ events. Black dots indicate donor cells, and gray dots indicate recipient cells. Data are representative of three independent experiment, with n = 1 mouse/experiment per time point.

CD226⁻ MHC II⁺ macrophages 2.5 d after transfer and CD226⁺ MHC II⁺ macrophages 4 d after transfer (Fig. 3 F). We conclude that CD226⁺ macrophages and MHC II⁺ CD226⁻ macrophages of peritoneal and pleural cavities derive from blood monocytes not just postnatally but also in adults.

Antibiotic treatment and loss of IRF4 blocks differentiation of CD226⁺ macrophages

Transcriptional regulators that control the development and maintenance of MHC II⁺ macrophages in the peritoneal and pleural cavities are unknown. Our microarray data identified interferon regulatory factor 4 (IRF4) as a candidate to control peritoneal MHC II⁺ macrophages, as it was one of few transcription factors that distinguished this subset from other macrophages (Fig. 1 A and Table S1). Thus, we studied whole-body IRF4-deficient mice or conditional IRF4-deficient mice with IRF4 deletion driven by the CD11c promoter (CD11cCre × IRF4$^{fl/fl}$). The percentage and absolute numbers of peritoneal MHC II⁺ macrophages were reduced, whereas F4/80⁺ ICAM2⁺ macrophages were unaffected in the absence of IRF4 (Fig. 4, A and B). Strikingly, CD226⁺ macrophages within the MHC II⁺ macrophage subpopulation were not detected in the peritoneal cavity, indicating that they are completely dependent on IRF4. However, the number of CD226⁻ macrophages was unchanged in the absence or presence of IRF4, suggesting the CD226⁻ population was not regulated by IRF4 (Fig. 4, A and C). Blood monocyte counts were also normal in IRF4$^{-/-}$ mice (Fig. 4 D). Possibly, IRF4 regulates the progressive differentiation of the CD226⁻ population into the CD226⁺ macrophage.

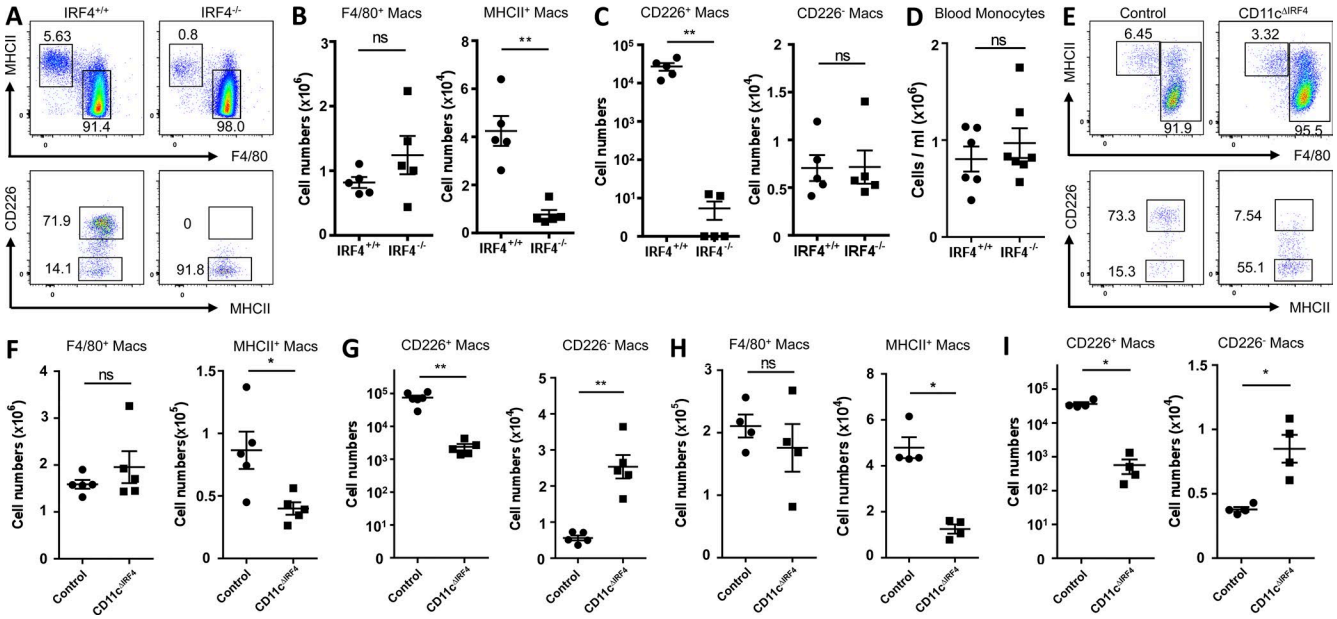

Figure 4. **IRF4 governs the development of CD226$^+$ macrophages.** (A) Flow cytometric analysis of F4/80$^+$ ICAM2$^+$ and MHC II$^+$ macrophage subpopulations in IRF4$^{+/+}$ and IRF4$^{-/-}$ mice. (B–D) Quantification of peritoneal F4/80$^+$ macrophages and MHC II$^+$ macrophages (B), MHC II$^+$ macrophage subpopulations (C), and blood monocytes (D) in IRF4$^{+/+}$ and IRF4$^{-/-}$ mice. Data are from two independent experiments (n = 5–7, mean ± SEM). P-values, unpaired Student's t test: **, P < 0.01. (E) Flow cytometric analysis of F4/80$^+$ ICAM2$^+$ macrophages and MHC II$^+$ macrophage subpopulations in peritoneal cavities of CD11c$^{\Delta IRF4}$ mice and controls that were Cre$^-$ IRF4$^{fl/fl}$ littermates or age- and sex-matched Cre$^+$ mice not bearing IRF4 floxed alleles. (F and G) Quantification of F4/80$^+$ macrophages and MHC II$^+$ macrophages (F) and MHC II$^+$ macrophage CC226$^-$ or CD226$^+$ subpopulations (G) in peritoneal cavities of CD11c$^{\Delta IRF4}$ mice (ΔIRF4) and controls. (H and I) Quantification of F4/80$^+$ ICAM2$^+$ or MHC II$^+$ macrophages (H) and MHC II$^+$ macrophage subpopulations (I) in pleural cavities of CD11c$^{\Delta IRF4}$ mice (ΔIRF4) and controls. (F–I) Data are representative of three independent experiments (n = 3–4 mice/experiment, mean ± SEM). P-values, unpaired Student's t test: *, P < 0.05; **, P < 0.01.

We also analyzed mice expressing Cre recombinase driven by CD11c promoter crossed with mice bearing floxed IRF4 alleles. Flow cytometric analysis showed peritoneal F4/80^{hi} macrophages were not affected by IRF4 deficiency in CD11c^{cre} × IRF4$^{fl/fl}$ (CD11c$^{\Delta IRF4}$) mice. However, the number of MHC II$^+$ macrophages was significantly reduced in CD11c$^{\Delta IRF4}$ mice compared with littermate control mice lacking Cre or age-matched Cre$^+$ mice carrying nonfloxed IRF4 alleles (Fig. 4, E and F). Similar to IRF4$^{-/-}$ mice, peritoneal CD226$^+$ macrophages gated on MHC II$^+$ macrophages were significantly reduced in CD11c$^{\Delta IRF4}$mice, whereas the number of MHC II$^+$ CD226$^-$ macrophages was increased (Fig. 4, E and G). A similar pattern was observed in the pleural cavity (Fig. 4, H and I). These data support the conclusion that IRF4 controls the development or persistence of MHC II$^+$ CD226$^+$ macrophages even though their precursors in blood and MHC II$^+$ CD226$^-$ macrophages that serve as their immediate precursors do not depend on IRF4.

Finally, although the function of CD226$^+$ macrophages remains unknown, we considered the possibility that microbial exposure after birth and continuously in adulthood might generate signals driving ongoing monocyte recruitment and differentiation to CD226$^+$ macrophages. We thus wondered whether this subset of macrophages in adult mice might be eliminated by antibiotics. Indeed, whereas the number of F4/80$^+$ ICAM2$^+$ macrophages remained unaffected by oral antibiotics, MHC II$^+$ macrophages were markedly reduced (Fig. 5 A), following a similar pattern as observed with IRF4 deficiency in which a relative accumulation of CD226$^-$ macrophages with especially marked loss of CD226$^+$ macrophages was apparent (Fig. 5 B). However, the number of Ly-6C^{hi} monocytes in the blood was unaffected (Fig. 5 C). Thus, we conclude that the differentiation of CD226$^+$ peritoneal macrophages from CD226$^-$ macrophages, derived from infiltrating monocytes, may be driven not only by IRF4 but also by microbial exposure that in turn is suppressed by antibiotic treatment. Clearly, the relationship between the F4/80$^+$ and MHC II$^+$ peritoneal and pleural macrophage subpopulations in each compartment is distinct. Future studies are now needed to determine whether CD226$^+$ macrophages are crucial in host defense and whether microbial signals drive expression of IRF4 within their precursors.

MATERIALS AND METHODS

Mouse strains

Mice were housed in specific pathogen–free barrier facilities, maintained by the Division of Comparative Medicine, Washington University School of Medicine. CD226$^{-/-}$ mice (Gilfillan et al., 2008) and CCR2$^{GFP/+}$ mice (Satpathy et al., 2013) were generated as previously described. CX$_3$CR1^{CreER}

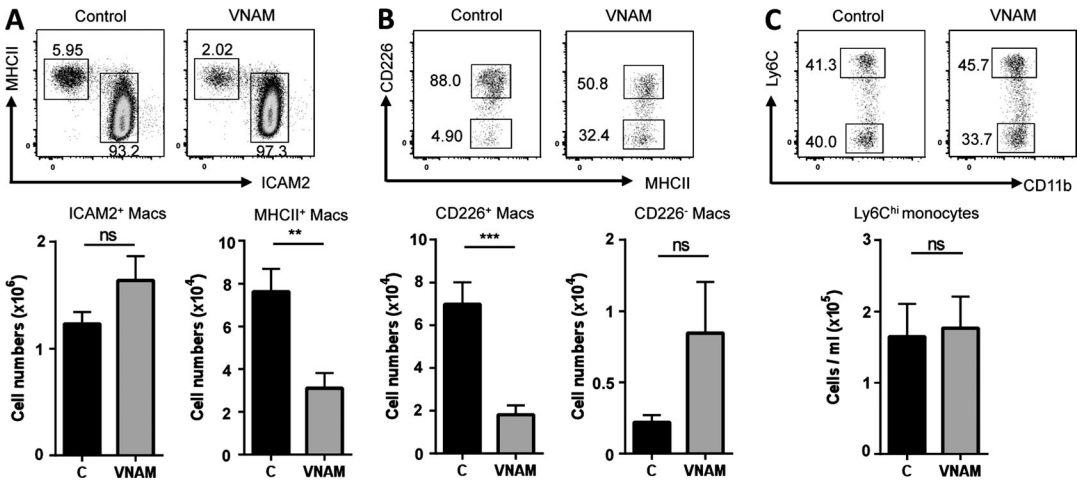

Figure 5. **Antibiotic sensitivity of CD226$^+$ macrophages.** (A and B) Flow cytometric analysis and quantification (below) of F4/80$^+$ ICAM2$^+$ and MHC II$^+$ macrophages (A) or MHC II$^+$ macrophage subpopulations (B) in the presence of antibiotic treatment (VNAM) or its absence ("C" for control group). Data are pooled from four independent experiments (n = 14–15/group, mean ± SEM). (C) Flow cytometric analysis of monocyte subpopulations and quantification (below) of Ly6C^{hi} monocytes. Data are pooled from three independent experiments (n = 8/group, mean ± SEM). P-values, unpaired Student's t test: **, P < 0.01; ***, P < 0.001.

mice were reconstituted from the cryopreserved sperm provided from S. Jung (Weizmann Institute of Science, Rehovot, Israel; Yona et al., 2013), and IRF4$^{-/-}$ mice were a gift from K.M. Murphy (Washington University School of Medicine, St. Louis, MO). CD11c-EYFP mice (B6.Cg-Tg(Itgax-Venus)1Mnz/J; Lindquist et al., 2004), Rosa26TdTomato mice (B6.Cg-Gt(Rosa)*26Sor*$^{tm14(CAG-TdTomato)Hze}$/J; Madisen et al., 2010), CD45.1 mice (B6.SJL-*PtPrc*^{a}*PePc*^{b}/BoyJ), CX$_3$CR1$^{gfp/+}$ mice (B5.129P(Cg)-*Ptprc*^{a} CX$_3$CR1^{tm1Litt}/LittJ; Jung et al., 2000), CD11c^{Cre} mice (B6.Cg-Tg(Itgax-cre)1-1Reiz/J; Caton et al., 2007), IRF4^{flox} mice (B6.129S1-Irf4$^{tm-1Rdf/J}$; Klein et al., 2006), and CCR2$^{-/-}$ mice (Ccr2$^{tm1/fc}$; Boring et al., 1997) were purchased from The Jackson Laboratory. All experimental procedures were approved by the Animal Studies Committee at Washington University School of Medicine.

Microarray analysis

Macrophage purifications and Affymetrix-based microarray analysis were performed as part of the Immunological Genome Project, as previously described (Gautier et al., 2012). In the ImmGen database, small MHC II$^+$ macrophages are annotated as MF.II+480lo.PC, and their expression profile can be searched at http://www.immgen.org. Here, we performed new analysis of this existing, highly standardized dataset. The GEO accession code for these data is GSE15907. In the present analysis, all unannotated genes were excluded. For genes with multiple transcripts in the array set, the one with the highest intensity was chosen to carry through the analysis. This left 18,616 transcripts available for comparison. We then used a Student's t test to find differences between MHC II$^+$ peritoneal macrophages and all other macrophage populations in the comparison (F4/80$^+$ peritoneal macrophages, lung macrophages, brain [central nervous system] macrophages, and red pulp macrophages from the spleen). Bonferroni correction for multiple comparisons was then applied. Using this approach, only comparisons with a Student's t test with a p-value $<2.69 \times 10^{-6}$ were carried forward. Probes with a signal intensity <120 across all populations indicated those not expressed in any macrophages; these were removed. 112 genes were deemed to be highly expressed in MHC II$^+$ resident peritoneal macrophages but not others, by a factor of 1.8–99-fold. The full list of these differences can be found in Table S1.

Cell isolation and quantification of peritoneal and pleural macrophages

Peritoneal cells were harvested after a 5-ml injection of HBSS containing 2 mM EDTA and 2% FBS into the peritoneal space. Peritoneal cells of pups were harvested by 50–100-µl injection of HBSS containing 2 mM EDTA and 2% FBS into peritoneal space with insulin syringe (29 1/2G). In the pups, peritoneal cell harvest was repeated two to three times, and the lavage from each wash combined. Pleural cells were harvested after a 0.8–1-ml injection of HBSS containing 2 mM EDTA and 2% FBS into the pleural space. For the analysis of blood monocytes, 200–300 µl of peripheral blood was collected from puncture of the submandibular cheek vessel; then red blood cells were removed with lysis buffer (BD). Total peritoneal and pleural macrophages, or total leukocytes in blood, were counted by using an automated cell counter (Nexcelom). Then this number was multiplied by the percentage of CD11b$^+$ CD115$^+$ macrophages stained for large macrophage markers ICAM2 and F4/80 or small macrophage markers MHC II and CD226, as analyzed by flow cytometry. Monocytes were stained with anti-CD45, anti-CD11b, anti-CD115, and anti-Ly6C.

Antibodies and flow cytometric analysis

The following antibodies were purchased from BioLegend: anti-CD11b (M1/70), anti-CD102 (ICAM2; 3C4; MIC2/4), anti-F4/80 (BM8), anti–MHC II (I-A/I-E; M5/114.15.2), anti-CD226 (DNAM-1; 10E5), anti-CD45 (30-F11), anti-CD11c (N418), anti-Ly6C (HK1.4), anti-CD45.2 (104), anti-Ly6G (1A8), and anti-CD19 (6D5). These antibodies were purchased from eBioscience: CD115 (AFS98), anti-CD4 (RM4-5), anti-CD8a (53-6.7), anti-CD45.1 (A20), TCR-β (H57-597), and anti-CD3e (145-2C11). Cells were analyzed on Fortessa or LSR II (BD) flow cytometers, and data were analyzed with FlowJo software (Tree Star).

Fate mapping study

CX_3CR1^{CreER} mice were crossed onto $Rosa26^{Tomato}$ mice. To induce the cre recombination fused with estrogen receptor, tamoxifen-enriched diet was purchased from Envigo and fed ad libitum to CX_3CR1^{CreER}:$Rosa26^{Tomato}$ mice for 3 wk before the execution of experiments.

Parabiosis approach

Parabiotic mice were produced as described previously (Liu et al., 2009). In brief, mice were shaved. 3 d later, an incision in the skin extending from the knee of hind leg to elbow and ligament of forepaw was made and then sutured with the skin of another mouse bearing a similar incision. Sutures were closed with 7-mm and 9-mm stainless steel wound clips. Mice were treated with 150 µl buprenorphine (30 µg/ml) mixed with 500 µl of 5% dextrose for pain relief. Antibiotic-treated water was provided for 3 wk after the surgery to prevent infections. Wound clips were removed after 2 wk after the surgery.

Adoptive transfer of monocytes

Splenocytes from $CD45.2^+$ $CCR2^{gfp/+}$ mice were filtered through a 70-µm strainer, and red blood cells were removed by lysis buffer (BD). Taking advantage of biotinylated anti-CD115 antibody (eBioscience) and streptavidin-magnetic microbeads (Miltenyi Biotech), splenic monocytes were enriched using a MACS LS column. Cells were stained with anti-CD11b, anti-CD115, and anti-Ly6C antibodies, and $Ly6C^{hi}$ monocytes expressing GFP were sorted using a FACSAria II system (BD). Sorted cells (>95% purity) were injected i.v. into congenic CD45.1 mice (1.2×10^6 cells/mouse). Recipient mice were sacrificed and analyzed at day 2.5 or day 4 after injection.

Antibiotic treatment

Adult C57BL/6 mice were treated orally with a combination of broad-spectrum antibiotics, as previously described (Baldridge et al., 2015): vancomycin (0.5 g/liter; Sigma-Aldrich), neomycin (1 g/liter; Sigma-Aldrich), ampicillin (1 g/liter; Sigma-Aldrich), and metronidazole (1 g/liter; MP Biomedicals) dissolved in grape Kool-Aid (20 g/liter; Kraft Foods). This solution was substituted for drinking water for 2–3 wk before euthanasia and cell analysis; control mice received the grape Kool-Aid without antibiotics.

Statistical analysis

The statistical significance of differences in mean values was analyzed by unpaired, two-tailed Student's *t* test or ANOVA for multiple comparisons using Prism software (GraphPad Software), as indicated in each legend. P-values <0.05 were considered statistically significant. Error bars show the SEM.

Online supplemental material

Table S1 lists all mRNA transcripts that were statistically significantly elevated in peritoneal MHC II^+ small macrophages from the Immunological Genome Project database, using the method for analysis described in Materials and methods. Online supplemental material is available at http://www.jem.org/cgi/content/full/jem.20160486/DC1.

ACKNOWLEDGMENTS

This work was supported by National Institutes of Health (NIH) grants R01 AI049653, R21 AG046734, R01 HL118206, and DP1DK109668 to G.J. Randolph. J.W. Williams was supported by NIH training grant 2T32DK007120-41.

The authors declare no competing financial interests.

Submitted: 4 April 2016
Accepted: 12 July 2016

REFERENCES

Baldridge, M.T., T.J. Nice, B.T. McCune, C.C. Yokoyama, A. Kambal, M. Wheadon, M.S. Diamond, Y. Ivanova, M. Artyomov, and H.W. Virgin. 2015. Commensal microbes and interferon-λ determine persistence of enteric murine norovirus infection. *Science.* 347:266–269. http://dx.doi.org/10.1126/science.1258025

Boring, L., J. Gosling, S.W. Chensue, S.L. Kunkel, R.V. Farese Jr., H.E. Broxmeyer, and I.F. Charo. 1997. Impaired monocyte migration and reduced type 1 (Th1) cytokine responses in C-C chemokine receptor 2 knockout mice. *J. Clin. Invest.* 100:2552–2561. http://dx.doi.org/10.1172/JCI119798

Cain, D.W., E.G. O'Koren, M.J. Kan, M. Womble, G.D. Sempowski, K. Hopper, M.D. Gunn, and G. Kelsoe. 2013. Identification of a tissue-specific, C/EBPβ-dependent pathway of differentiation for murine peritoneal macrophages. *J. Immunol.* 191:4665–4675. http://dx.doi.org/10.4049/jimmunol.1300581

Caton, M.L., M.R. Smith-Raska, and B. Reizis. 2007. Notch–RBP-J signaling controls the homeostasis of $CD8^-$ dendritic cells in the spleen. *J. Exp. Med.* 204:1653–1664. http://dx.doi.org/10.1084/jem.20062648

Epelman, S., K.J. Lavine, A.E. Beaudin, D.K. Sojka, J.A. Carrero, B. Calderon, T. Brija, E.L. Gautier, S. Ivanov, A.T. Satpathy, et al. 2014a. Embryonic and adult-derived resident cardiac macrophages are maintained through distinct mechanisms at steady state and during inflammation. *Immunity.* 40:91–104. http://dx.doi.org/10.1016/j.immuni.2013.11.019

Epelman, S., K.J. Lavine, and G.J. Randolph. 2014b. Origin and functions of tissue macrophages. *Immunity.* 41:21–35. http://dx.doi.org/10.1016/j.immuni.2014.06.013

Gautier, E.L., T. Shay, J. Miller, M. Greter, C. Jakubzick, S. Ivanov, J. Helft, A. Chow, K.G. Elpek, S. Gordonov, et al. Immunological Genome Consortium. 2012. Gene-expression profiles and transcriptional regulatory pathways that underlie the identity and diversity of mouse tissue macrophages. *Nat. Immunol.* 13:1118–1128. http://dx.doi.org/10.1038/ni.2419

Gautier, E.L., S. Ivanov, J.W. Williams, S.C. Huang, G. Marcelin, K. Fairfax, P.L. Wang, J.S. Francis, P. Leone, D.B. Wilson, et al. 2014. Gata6 regulates aspartoacylase expression in resident peritoneal macrophages and controls their survival. *J. Exp. Med.* 211:1525–1531. http://dx.doi.org/10.1084/jem.20140570

Geissmann, F., S. Jung, and D.R. Littman. 2003. Blood monocytes consist of two principal subsets with distinct migratory properties. *Immunity.* 19:71–82. http://dx.doi.org/10.1016/S1074-7613(03)00174-2

Ghosn, E.E., A.A. Cassado, G.R. Govoni, T. Fukuhara, Y. Yang, D.M. Monack, K.R. Bortoluci, S.R. Almeida, L.A. Herzenberg, and L.A. Herzenberg. 2010. Two physically, functionally, and developmentally distinct peritoneal macrophage subsets. *Proc. Natl. Acad. Sci. USA.* 107:2568–2573. http://dx.doi.org/10.1073/pnas.0915000107

Gilfillan, S., C.J. Chan, M. Cella, N.M. Haynes, A.S. Rapaport, K.S. Boles, D.M. Andrews, M.J. Smyth, and M. Colonna. 2008. DNAM-1 promotes activation of cytotoxic lymphocytes by nonprofessional antigen-presenting cells and tumors. *J. Exp. Med.* 205:2965–2973. http://dx.doi.org/10.1084/jem.20081752

Ginhoux, F., and M. Guilliams. 2016. Tissue-resident macrophage ontogeny and homeostasis. *Immunity.* 44:439–449. http://dx.doi.org/10.1016/j.immuni.2016.02.024

Hashimoto, D., A. Chow, C. Noizat, P. Teo, M.B. Beasley, M. Leboeuf, C.D. Becker, P. See, J. Price, D. Lucas, et al. 2013. Tissue-resident macrophages self-maintain locally throughout adult life with minimal contribution from circulating monocytes. *Immunity.* 38:792–804. http://dx.doi.org/10.1016/j.immuni.2013.04.004

Ingersoll, M.A., R. Spanbroek, C. Lottaz, E.L. Gautier, M. Frankenberger, R. Hoffmann, R. Lang, M. Haniffa, M. Collin, F. Tacke, et al. 2010. Comparison of gene expression profiles between human and mouse monocyte subsets. *Blood.* 115:e10–e19. http://dx.doi.org/10.1182/blood-2009-07-235028

Jung, S., J. Aliberti, P. Graemmel, M.J. Sunshine, G.W. Kreutzberg, A. Sher, and D.R. Littman. 2000. Analysis of fractalkine receptor CX_3CR1 function by targeted deletion and green fluorescent protein reporter gene insertion. *Mol. Cell. Biol.* 20:4106–4114. http://dx.doi.org/10.1128/MCB.20.11.4106-4114.2000

Klein, U., S. Casola, G. Cattoretti, Q. Shen, M. Lia, T. Mo, T. Ludwig, K. Rajewsky, and R. Dalla-Favera. 2006. Transcription factor IRF4 controls plasma cell differentiation and class-switch recombination. *Nat. Immunol.* 7:773–782. http://dx.doi.org/10.1038/ni1357

Lavin, Y., A. Mortha, A. Rahman, and M. Merad. 2015. Regulation of macrophage development and function in peripheral tissues. *Nat. Rev. Immunol.* 15:731–744. http://dx.doi.org/10.1038/nri3920

Lindquist, R.L., G. Shakhar, D. Dudziak, H. Wardemann, T. Eisenreich, M.L. Dustin, and M.C. Nussenzweig. 2004. Visualizing dendritic cell networks in vivo. *Nat. Immunol.* 5:1243–1250. http://dx.doi.org/10.1038/ni1139

Liu, K., G.D. Victora, T.A. Schwickert, P. Guermonprez, M.M. Meredith, K. Yao, F.F. Chu, G.J. Randolph, A.Y. Rudensky, and M. Nussenzweig. 2009. In vivo analysis of dendritic cell development and homeostasis. *Science.* 324:392–397. http://dx.doi.org/10.1126/science.1170540

Madisen, L., T.A. Zwingman, S.M. Sunkin, S.W. Oh, H.A. Zariwala, H. Gu, L.L. Ng, R.D. Palmiter, M.J. Hawrylycz, A.R. Jones, et al. 2010. A robust and high-throughput Cre reporting and characterization system for the whole mouse brain. *Nat. Neurosci.* 13:133–140. http://dx.doi.org/10.1038/nn.2467

Molawi, K., Y. Wolf, P.K. Kandalla, J. Favret, N. Hagemeyer, K. Frenzel, A.R. Pinto, K. Klapproth, S. Henri, B. Malissen, et al. 2014. Progressive replacement of embryo-derived cardiac macrophages with age. *J. Exp. Med.* 211:2151–2158. http://dx.doi.org/10.1084/jem.20140639

Newson, J., M. Stables, E. Karra, F. Arce-Vargas, S. Quezada, M. Motwani, M. Mack, S. Yona, T. Audzevich, and D.W. Gilroy. 2014. Resolution of acute inflammation bridges the gap between innate and adaptive immunity. *Blood.* 124:1748–1764. http://dx.doi.org/10.1182/blood-2014-03-562710

Okabe, Y., and R. Medzhitov. 2014. Tissue-specific signals control reversible program of localization and functional polarization of macrophages. *Cell.* 157:832–844. http://dx.doi.org/10.1016/j.cell.2014.04.016

Rosas, M., L.C. Davies, P.J. Giles, C.T. Liao, B. Kharfan, T.C. Stone, V.B. O'Donnell, D.J. Fraser, S.A. Jones, and P.R. Taylor. 2014. The transcription factor Gata6 links tissue macrophage phenotype and proliferative renewal. *Science.* 344:645–648. http://dx.doi.org/10.1126/science.1251414

Satpathy, A.T., C.G. Briseño, J.S. Lee, D. Ng, N.A. Manieri, W. Kc, X. Wu, S.R. Thomas, W.L. Lee, M. Turkoz, et al. 2013. Notch2-dependent classical dendritic cells orchestrate intestinal immunity to attaching-and-effacing bacterial pathogens. *Nat. Immunol.* 14:937–948. http://dx.doi.org/10.1038/ni.2679

Schneider, C., S.P. Nobs, M. Kurrer, H. Rehrauer, C. Thiele, and M. Kopf. 2014. Induction of the nuclear receptor PPAR-γ by the cytokine GM-CSF is critical for the differentiation of fetal monocytes into alveolar macrophages. *Nat. Immunol.* 15:1026–1037. http://dx.doi.org/10.1038/ni.3005

Schulz, C., E. Gomez Perdiguero, L. Chorro, H. Szabo-Rogers, N. Cagnard, K. Kierdorf, M. Prinz, B. Wu, S.E. Jacobsen, J.W. Pollard, et al. 2012. A lineage of myeloid cells independent of Myb and hematopoietic stem cells. *Science.* 336:86–90. http://dx.doi.org/10.1126/science.1219179

Serbina, N.V., and E.G. Pamer. 2006. Monocyte emigration from bone marrow during bacterial infection requires signals mediated by chemokine receptor CCR2. *Nat. Immunol.* 7:311–317. http://dx.doi.org/10.1038/ni1309

Tamoutounour, S., M. Guilliams, F. Montanana Sanchis, H. Liu, D. Terhorst, C. Malosse, E. Pollet, L. Ardouin, H. Luche, C. Sanchez, et al. 2013. Origins and functional specialization of macrophages and of conventional and monocyte-derived dendritic cells in mouse skin. *Immunity.* 39:925–938. http://dx.doi.org/10.1016/j.immuni.2013.10.004

Yona, S., K.W. Kim, Y. Wolf, A. Mildner, D. Varol, M. Breker, D. Strauss-Ayali, S. Viukov, M. Guilliams, A. Misharin, et al. 2013. Fate mapping reveals origins and dynamics of monocytes and tissue macrophages under homeostasis. *Immunity.* 38:79–91. (published erratum appears in *Immunity*. 2013. 38:1073–1079.) http://dx.doi.org/10.1016/j.immuni.2012.12.001